Short Communication

A Novel Composite Anode Material of Si-SnO$_2$-graphene Prepared in Air for Lithium Ion Batteries

Chenxue Li[1], Yuhong Chen[2,*], Binjuan Wei[1], Keqiang Ding[1,*], Yan Zhang[1], Xiaomi Shi[1], Jinming Zhou[1,*]

[1] College of Chemistry and Materials Science, Hebei Normal University, Shijiazhuang, Hebei 050024, P.R. China
[2] Department of Chemical and Environmental Engineering, Hebei Chemical & Pharmaceutical Vocational Technology College, Shijiazhuang 050026.
[*]E-mail: dkeqiang@263.net, chyh76@163.com, zhoujm@iccas.ac.cn

For the first time, a novel composite material, that contained Si, SnO$_2$ and graphene, was prepared by using an air condition calcination method employing commercial silicon wafer, SnCl$_4$ and graphene as the starting materials. In this work, four samples, i.e., Si (sample a), Si+SnCl$_4$ (sample b), Si+SnCl$_4$+graphene (sample c) and Si+SnCl$_4$+lignin (sample d), were fabricated and systematically investigated. The physicochemical properties of the synthesized samples were characterized mainly by using X-ray diffraction (XRD) and scanning electron microscopy (SEM). XRD results strongly indicated that elementary Si existed in all prepared samples and SnO$_2$ was contained in sample b, c and d. The electrochemical properties of the resultants samples were investigated basically by employing cyclic voltammometry (CV), galvanostatic charge-discharge tests and electrochemical impedance spectroscopy (EIS), and the results revealed that the discharge capacities of sample c and d were respectively estimated to be about 350 and 272 mAh g^{-1} after 20 cycles at 100 mA g^{-1}. It should be emphasized that no harsh preparation conditions were employed in this work. That is to say, this newly created novel kind of composite anode materials, i.e., sample c, can be large-scale produced easily, being very helpful to the development of commercial production of lithium ions batteries (LIBs) anode materials.

1. INTRODUCTION

Recently, the following drawbacks of using graphite as the anode material for lithium ion batteries(LIBs) have been urgently claimed [1,2], (1) The theoretical capacity of graphite (372 mAh g$^-$

[1]) is lower which cannot meet the demand of producing LIBs with higher energy density. (2) The growth of metallic Li dendrite on the surface of graphite is unavoidable especially when being overcharged, which generally leads to safety issue such as the short circuit and thermal runaway. (3) Some unstable solid-electrolyte interfaces (SEI) can be easily formed on the surface of graphite due to the decomposition of electrolyte, because of the fact that the electrode potential of graphite is commonly lower than that of Li-ion battery electrolytes. Therefore, creating a novel anode material, which has some superior properties such as longer cycle life, higher energy density and higher rate capability, is still a major task for the LIBs-related researchers [3, 4].

To our knowledge, except for novel kinds of carbon [5], two typical novel kinds of anode materials, namely, some transition metal oxides [6] and some elementary substances [7], have been developed for LIBs in recent years. Among those metal oxides based substances, SnO_2 has been widely investigated as anode material for LIBs mainly due to its higher theoretical capacity (1494 mAh g^{-1}) and rich reserves [8]. For example, in 2017, Yuan's group reported the synthesis of reduced graphene oxide supported fluorine-doped SnO_2 as anode material for LIBs, and they thought that the improved electrochemical performances such as the higher capacity, better long-term cycling stability and superior rate capability were mainly benefited from the improved electrical conductivity and enhanced Li-ion diffusion ability[9]. It should be noted that in Yuan's work the annealing treatment was completed in an oxygen-free atmosphere, which was rather different from our work reported in this communication. Among the elementary substances, silicon (Si) was regarded as one promising anode material of LIBs mostly because of its higher theoretical capacity (4200 mAh g^{-1}), low cost and environmental benignity [10, 11]. For instance, Lu's group [12] prepared a Si-based multi-component three-dimensional (3D) network using a facile high energy ball-milling method, and for the synthesized samples, the Si cores were capped with phytic acid shell layers. Although as mentioned above, many novel kinds of anode materials have been produced showing relatively improved electrochemical performance, the practical applications of these novel anode materials in LIBs are very rare. Generally, the lower electrical conductivity and the severe pulverization were thought as the main two issues which greatly hindered the further applications of those newly developed anode materials in LIBs. Or in other words, developing novel high performance anode materials is still a main topic in the research works concerning LIBs.

In this work, commercial silicon wafer, $SnCl_4$ and graphene were employed as the starting materials, and four kinds of samples were prepared using a very facile air condition calcination method. Namely, four samples, i.e., Si, $Si+SnCl_4$, $Si+SnCl_4+graphene$ and $Si+SnCl_4+lignin$, were fabricated and systematically investigated. XRD results indicated that elementary silicon and SnO_2 were the main components of the later three samples. SEM images results demonstrated that, for sample b, c and d, Si particles were likely coated by SnO_2 particles, and some flakes of graphene were doped into sample c. Electrochemical measurement results revealed that the discharge capacity of sample c was evaluated to be about 350 mAh g^{-1} after 20 cycles at 100 mA g^{-1}, which was significantly larger than the theoretical capacity value of lithium titanate ($Li_4Ti_5O_{12}$ (1C=175 mAh g^{-1}), LTO).

2. EXPERIMENTAL

2.1. Materials

All chemicals were of analytical grade and purchased from Tianjin Chemical Reagent Co. Ltd. All materials used for the battery measurement were all bought from Tianjin Lianghuo S&T Developing Co. Ltd. It should be emphasized that all the chemicals were used as-received with no further purification.

2.2. Preparation of the samples

5 g silicon wafer was thoroughly milled in a ball grinder for 12 h generating silicon powders, which was nominated as sample a. A proper amount of $SnCl_4 \cdot 5H_2O$ was dissolved into 20 mL distilled water producing a solution, and then, a proper amount of as-prepared sample a was dispersed into above resultant solution, which was vigorously stirred at 70℃ for 3 h creating a suspension solution. It should be noted that the added amount of $SnCl_4 \cdot 5H_2O$ and silicon powders were on the basis of the atomic ratio of Sn to Si, and in this work, the atomic ratio of Sn to Si was 1:1. Subsequently, the prepared suspension solution was heated in an air dry oven at 150℃ for 4 h generating dry precursors. And lastly, the dry precursors were fully milled in an agate mortar for 30 min to produce powders, and then, the resulting powders were pressed into pieces, and the obtained pieces were calcined at 300℃ for 3h in a muffle furnace under air conditions to fabricate the samples. The prepared sample using above process was called as sample b.

In the preparation of sample c, after the addition of $SnCl_4 \cdot 5H_2O$ and silicon powders into 20mL distilled water, a proper amount of graphene was subsequently added into above 20mL distilled water. The added amounts of $SnCl_4 \cdot 5H_2O$ and silicon powders were respectively identical to that of preparing sample b. The weight percentage of graphene was about 3% of the total weight of the added $SnCl_4 \cdot 5H_2O$ and silicon powders. Other preparation processes were identical to that of sample b preparation. Evidently, the price of graphene was higher as compared to other kinds of carbon, thus, lignin, a traditional additive for lead acid battery, was employed to replace graphene in preparing sample d. In the case of sample d preparation, except for the utilization of lignin, no different preparation processes were employed compared to that of sample c preparation. Summarily, the samples with the starting materials of Si, Si+SnCl₄, Si +SnCl₄+graphene and Si +SnCl₄+ lignin were named as sample a, b, c and d, respectively.

2.3. Characterization

The crystal structures and compositions of the prepared samples were studied by using X-ray diffraction (Bruker AXS, D8 ADVANCE, Germany). Energy dispersive spectrometer (EDS, INCA Energy 350, England) was used to examine the element components of the produced samples. The morphologies of the synthesized samples were viewed by scanning electron microscopy (HITACHI, SEM S-570).

Electrochemical measurements mainly including cyclic voltammetry (CV) and electrochemical impedance spectroscopy (EIS) were conducted on a CHI 660B electrochemical workstation (Shanghai Chenhua Apparatus, China). In the EIS measurement, the frequency range of the alternating current (AC) was from 0.1 Hz to 100 kHz, with an oscillation voltage of 5 mV. All the experiments were performed at room temperature.

2.4. Preparation of the working electrode and the half-cells

To fabricate a working electrode, anode material contained slurries were made first. Namely, first of all, sample a, acetylene black and PVDF (polyvinylidene fluoride) were respectively weighted at a weight ratio of 8:1:1. And then, above three reagents were mixed together to produce a mixture. Subsequently, several drops of N-methylpyrrolidone were dropped into above prepared mixture which was followed by a thorough 10 min stirring, producing active material contained slurries. Soon afterwards, the obtained slurry was uniformly painted onto a Cu foil, which was, in a vacuum oven, dried at 120 °C for 6 h, producing a working electrode. The electrodes prepared using sample a, b, c and d were, respectively, nominated as electrode a, b, c and d.

The half-cell was assembled by one of above prepared working electrodes and a lithium metal foil, by which the battery properties of the synthesized samples were measured systematically. In the prepared half-cells, Celgard 2400 and 1 M $LiPF_6$ were used as the separator and the electrolyte, respectively. The solvent used in the synthesized half-cells was a mixed solvent which contained dimethyl carbonate (DMC), ethylene carbonate (EC), ethyl methyl carbonate (EMC) and vinylene Carbonate (VC). Evidently, the metallic lithium foil was utilized as both the reference and counter electrodes. The galvanostatic charge-discharge tests were carried out on a battery testing system (CT-3008W-5V20mA-S4, Shenzhen Neware Electronics Co., Ltd. China). In this preliminary work, the employed current densities were 100, 300, 500 and 700 mA g^{-1}, and the potential range was from 0 V to 3V.

3. RESULTS AND DISCUSSION

3.1 Characterizations of the samples

Fig.1 shows the XRD patterns of the synthesized samples, in which the standard XRD pattern for Si, SnO_2 and C are also displayed. Apparently, for all the samples, the typical diffraction peaks of Si [10] were clearly exhibited which strongly indicated the existence of elementary Si in the final samples. For sample b, c and d, the main diffraction peaks of SnO_2 [9] were also distinctly observed, which indicated that $SnCl_4$ in the starting materials has been converted into SnO_2 after the preparation process. For sample c and d, the presence of a broad diffraction peak at about 26° effectively demonstrated the existence of carbon in the final products basing on our previous work concerning graphene [13]. Careful observation also indicated that the highest diffraction peaks of the XRD pattern were displayed by sample c, which implied that sample c had a better crystal structure when compared

to other samples [14]. Generally, the well-defined crystal structure was favorable to the directional transfer of the electrons and ions in an electrode material basing on our former work regarding the electrode materials [15]. Thus, sample c probably can deliver a better electrochemical performance when compared to other samples.
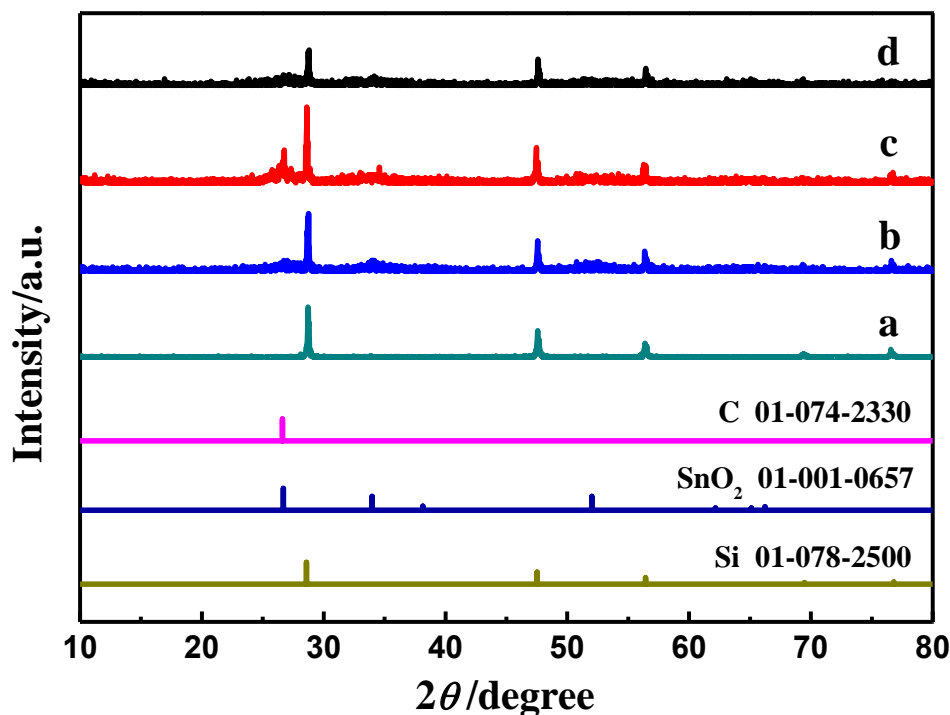
Figure 1. XRD patterns for the synthesized samples including the standard XRD patterns of Si, SnO_2 and C. Pattern a, b, c, and d is for sample a, b, c and d.
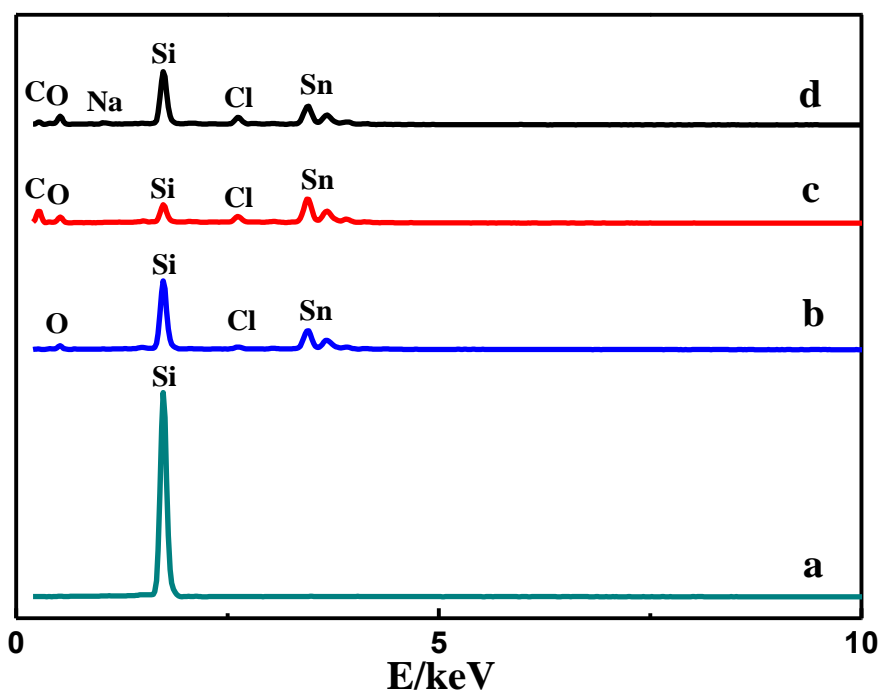
Figure 2. EDS spectra for all the produced samples. Curves a, b, c and d are for sample a, b, c and d.

The typical results of EDS examination are given in Fig.2. For sample a, only the element of Si was detected, which indicated no other impurities were introduced in the preparation process. In the case of sample b, the peaks corresponding to the elements of Si, Sn, Cl and O were all displayed clearly. The atomic content of Si, O, Sn and Cl in sample b was about 47.5%, 38.5%, 12.6% and 1.5%, respectively. The atomic ratio of Cl to Sn was about 0.12 rather than 4, which strongly indicated that more ions of Cl^- were lost in the preparation process. Also, this result demonstrated that more amounts of O were introduced in the preparation process. Apparently, the element of O should mainly exist in the form of metal oxide such as SnO_2. To our knowledge, it is difficult to oxidize Si to form SiO_2 under present preparation conditions. Meanwhile, for sample c and d, besides above elements, the element of C was detected which indicated that in the calcination process carbon in graphene and lignin was not totally consumed. The atomic content of Si, O, Sn, Cl and C in sample c and d was about 5.5% and 18.7%, 31.3% and 42.5%, 6.7% and 6.2%, 1.7% and 2.6%, 54.9% and 28.8%, respectively. Generally, the presence of carbon in the electrode materials was beneficial to the electrochemical performance improvement of an electrode material because of the higher electrical conductivity of carbon. That is to say, sample c and d should show better electrochemical performance as compared to other samples.
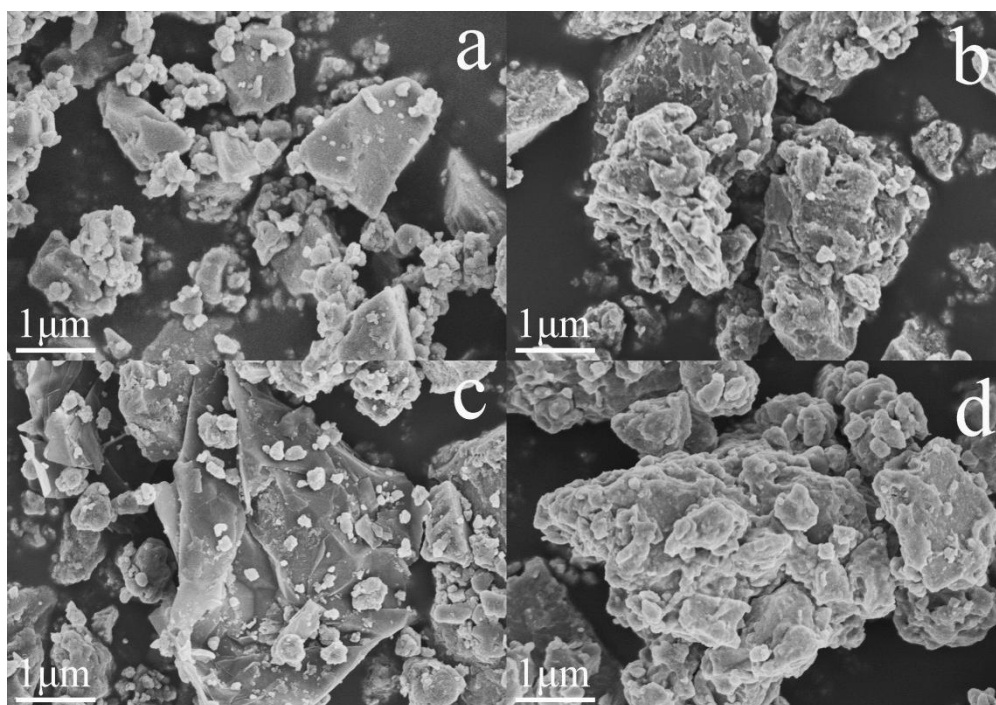
Figure 3. SEM images for all synthesized samples. Images a, b, c and d correspond to sample a, b c and d.

SEM images for all prepared samples are displayed in Fig.3. It is clear that for sample a, particles with various sizes and irregular shapes were seen clearly. While, as $SnCl_4$ was added in the starting materials, larger particles were prepared (image b). It indicated that, basing on the results of XRD pattern and EDS analysis, some prepared particles of SnO_2 were coated on the surface of sample a. Interestingly, for sample c, slice-like graphene was observed clearly, which indicated that in the

calcination process graphene was not totally burned by the oxygen gas in the air. It was reasonable to believe that in the calcination process, some oxygen gases reacted with $SnCl_4$ to produce SnO_2, instead of reacting with graphene to generate CO_2. Therefore, some graphenes with their original morphologies were retained in sample c. For sample d, larger particles with layered like structure were exhibited clearly which strongly indicated that some lignin were doped into the prepared samples. Meanwhile, according to the general scientific knowledge about Si, it could be confirmed that it was some difficult for Si to react with O_2 to produce oxides under such a mild reaction condition of 3h 300℃-calcination. Therefore, it could be speculated that in the prepared samples Si was employed as a core and the formed SnO_2 was coated on the surface of Si, as a result, particles with a core-shell structure were produced for sample b, c and d. Also, as shown by image c, for sample c, some pieces of graphene were inserted into those core-shell structure particles generating a so-called sandwiched structure.

3.2 Electrochemical properties
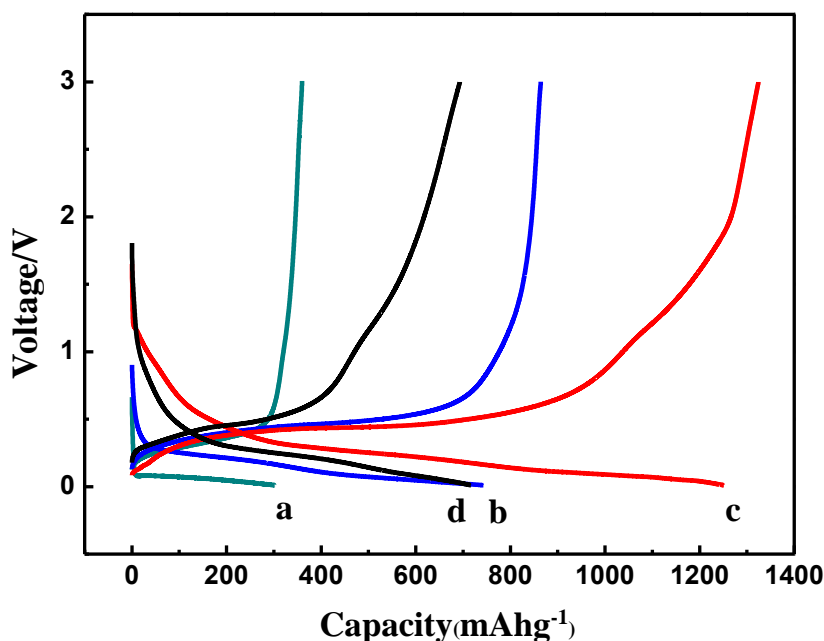
Figure 4. The initial galvanostatic charge-discharge plots in the potential range from 0V to 3V at 100 mA g^{-1}. Plots a, b, c and d were for the half-cells assembled by sample a, b, c and d.

The initial charge-discharge plots for all the half-cells, which were recorded at a current density of 100 mA g^{-1} in the potential range of 0-3 V, are illustrated in Fig.4. A sloped discharge voltage plateau accompanied by a relatively flat charging voltage plateau was seen for all half-cells. It should be noticed that the shapes of the charge-discharge plots shown in Fig.4 for electrode b, c and d were some different from that of both pure Si [16] and pure SnO_2 electrode [17]. That is to say, the charge-discharge processes in electrode b, c and d were a combined result. The results of Fig.4 effectively demonstrated that the insertion and extraction process of Li$^+$ could well proceed in all prepared

electrodes, though electrode a showed a very short discharge voltage plateau. The initial discharge capacity values for electrode a, b, c and d were roughly evaluated to be 306, 745, 1250 and 722 mAh g^{-1}, respectively. It should be emphasized that the discharge capacity of all the electrodes was remarkably larger than that of the theoretical discharge capacity of lithium titanate (LTO, 1C=175mAh g^{-1}) [18]. Obviously, electrode c, i.e., the sample of Si-SnO$_2$-graphene, delivered the largest discharge capacity value among all the prepared samples, which could only be attributed to the presence of graphene. Also, it was clear that except for electrode a, the discharge voltage plateau of all other three samples (about 0.28V vs. Li/Li$^+$) was greatly lower than that of LTO (around 1.5V vs. Li/Li$^+$) [19]. This result indicated that the output voltages of the LIBs using the prepared samples as anode materials would be much higher than that of those LIBs employing LTO as the anode materials when using the identical cathode materials and electrolyte, which may generate a higher power density.
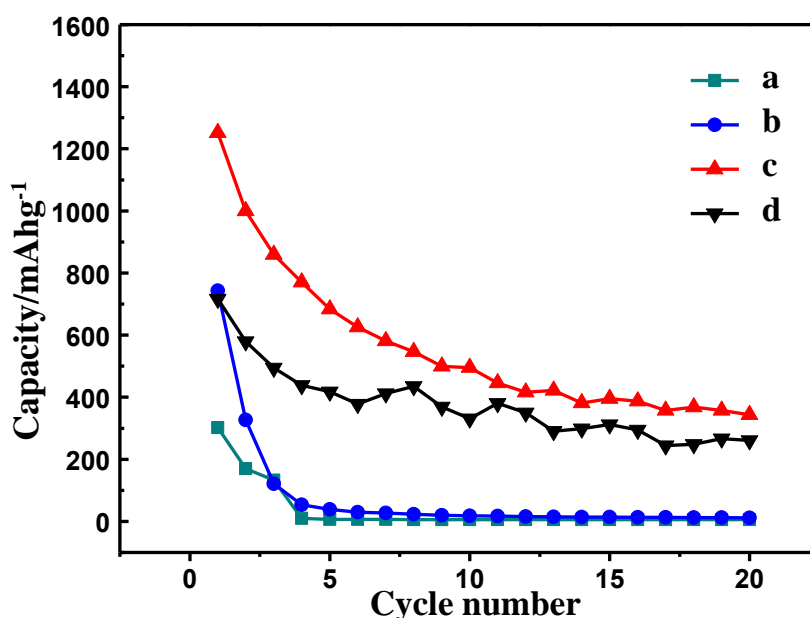
Figure 5. Cycling performances of all produced half-cells at 100 mA g^{-1}. Curves a, b, c and d were for the half-cells constructed by sample a, b, c and d.

It is well known that the cycling performance of an electrode material is a key factor which is closely related to the serve life of a LIB. The relationship between the discharge capacity and the cycling number for all prepared half-cells is described in Fig.5. Apparently, in all cases, the discharge capacity value decreased evidently with the cycle number, and electrode c showed the largest discharge capacity value among all the electrodes in the whole testing period. For example, the discharge capacities of the first cycle for electrode a, b, c and d were 306, 745, 1250 and 722 mAh g^{-1}, respectively. After 20 cycles, the discharge capacities for electrode a, b, c and d were estimated to be 0, 12, 350 and 263 mAh g^{-1}, respectively. This result definitely indicated that sample a and b could not be employed as anode material, and sample c and d could be used as anode materials instead. It seemed that carbon was a requisite factor in enhancing the electrochemical performance of the Si+SnO$_2$ composite anode material. Evidently, the amount of doped carbon as well as the doping method can

also significantly influence the electrochemical properties of the resultant anode materials, which will be investigated in detail in our subsequent research works.
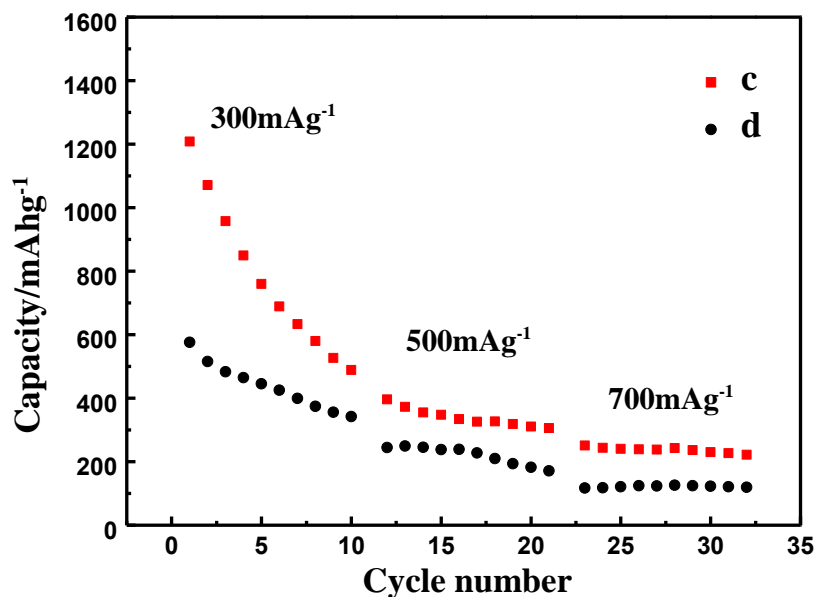
Figure 6. Rate capabilities of the produced half-cells at 300, 500, 700 mA g^{-1}. Curves c and d were for the half-cells constructed by sample c and d.
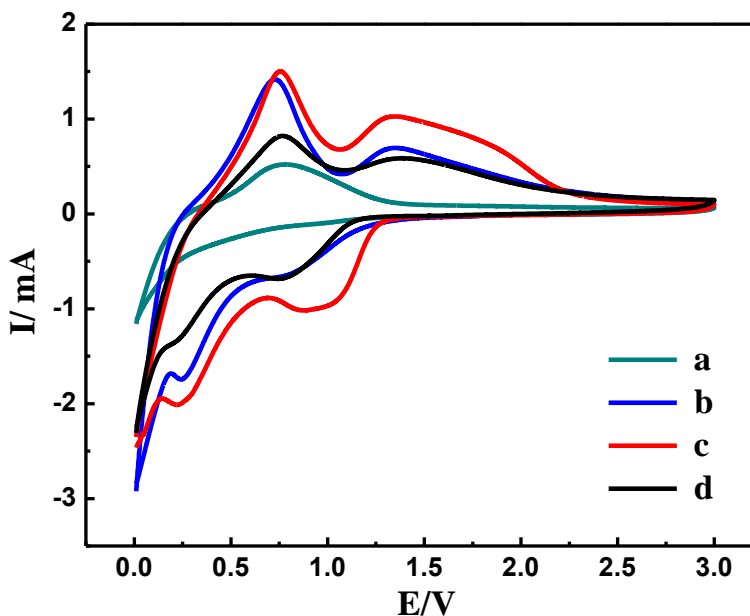
Figure 7. Cyclic voltammograms (CVs) of all the half-cells which were measured at 1 mV s^{-1}. Curve a, b, c and d were for the half-cells fabricated by sample a, b, c and d.

The rate capability of an electrode material is also a very important factor which will directly determine the charging or discharging time of a LIB, being closely related to the use efficiency of LIBs. Fig.6 shows the rate capabilities of electrode c and d, in which the half-cells were respectively

charged and discharged for 10 cycles under three current densities. Clearly, the discharge capacity value evidently decreased with increasing the applied current density, which was mainly due to the enhanced over-potential basing on the Tafel equation [19]. Interestingly, the discharge capacity of electrode c at the current density of 700 mA g^{-1} after 10 cycles was still maintained as high as 225 mAh g^{-1}, which was still larger than that of the theoretical discharge capacity of lithium titanate [18]. This result substantially indicated that sample c, i.e., the composite of Si-SnO$_2$-graphene, was a promising anode material for LIBs.

To better examine the insertion/extraction process of Li$^+$ in the prepared anode materials, CV curves for all prepared half-cells were recorded and shown in Fig.7. Generally, for a typical metallic Li -based two electrode half-cell, the electro-oxidation peak appearing in CV curves corresponded to a delithiation process in an electrode material, and the electro-reduction peak was resulted from a lithiation process. For electrode a, only an oxidation peak was observed which indicated that the lithiation and delithiation process in sample a was an irreversible process, which commonly led to poor electrochemical performance. While for other three samples, similar CV shape was displayed which probably indicated that sample b, c and d had a similar insertion/extraction process of Li$^+$. For electrode b, c and d, two oxidation peaks were respectively located at about 0.74V and 1.33V. And for electrode b and d, two reduction peaks were respectively positioned 0.24V and 0.80V. Interestingly, for electrode c, the first reduction peak was centered at 1.02V rather than at 0.80V, which strongly indicated that the doped graphene played a key role in reducing the over-potential, being very beneficial to the reversibility improvement of an anode material. Meanwhile, it was clear that the largest peak was displayed by electrode c, which demonstrated that the largest amount of Li$^+$ was transferred in the anode material of sample c.
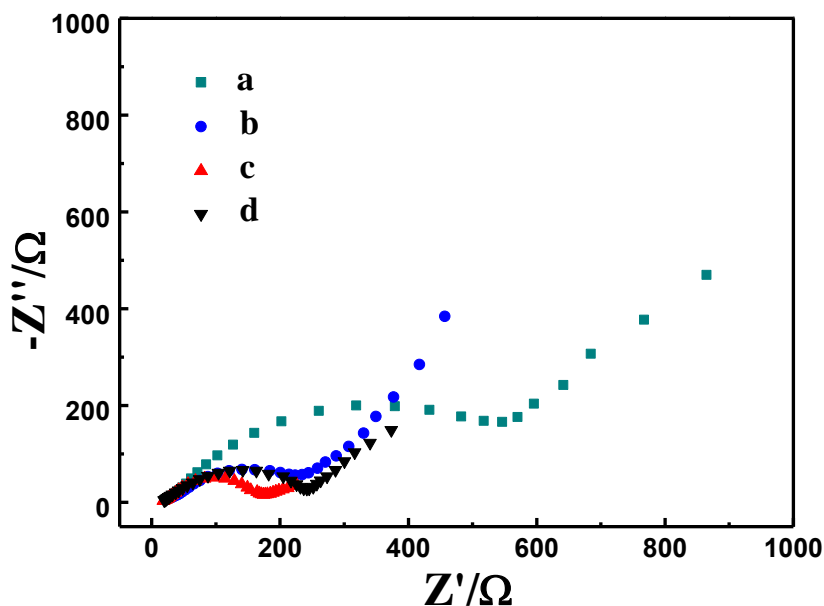
Figure 8. Nyquist plots of all prepared half-cells. Curves a, b, c and d were for the half-cells assembled by sample a, b, c and d.

Also, it should be noticed that the CV shapes of electrode b, c and d were very similar to that of the CV curves of the reduced graphene oxide supported fluorine-doped SnO_2 [9]. That is to say, the relatively higher capacity value delivered by above three samples was mainly attributed to the presence of anode material SnO_2. Detailed discussion will be conducted in our next report.

Electrochemical impedance spectroscopy (EIS) is a traditional electrochemical method, in which an alternating current with a frequency range was applied to a testing system. Among the various kinds of curves in EIS, Nyquist plot, due to its simple analysis, was the mostly used curve for analyzing a LIB. Fig. 8 shows the Nyquist plots of all produced half-cells. It should be emphasized that all the Nyquist curves were recorded at their open circuit potentials. Apparently, all the Nyquist plots were constructed by a semicircle in the higher frequency region and a 45° like line in the lower frequency region. Generally, the presence of the semicircle was originated from a parallel circuit that contained a resistor element and a capacitor element, and the diameter of the semicircle was approximately equal to the value of charge transfer resistance (R_{ct}), and the 45° line was generally closely related to the lithium-ion diffusion in the electrode materials [20]. Therefore, the values of R_{ct} were estimated to be about 630 Ω, 245 Ω, 185 Ω and 230 Ω for electrode a, b, c and d, respectively. This result effectively demonstrated that the doped carbon, namely, graphene and lignin, could remarkably reduce the value of R_{ct}, which was very favorable to the electrochemical performance improvement of the prepared electrode materials. Also, it can be seen clearly that electrode c showed the smallest value of R_{ct} among all the samples, which indicated that electrode c had the fastest kinetics among all prepared samples. This consequence accorded well with the results shown in Fig.4, 5 and 6, namely, sample c delivered the best electrochemical performance among these four samples.
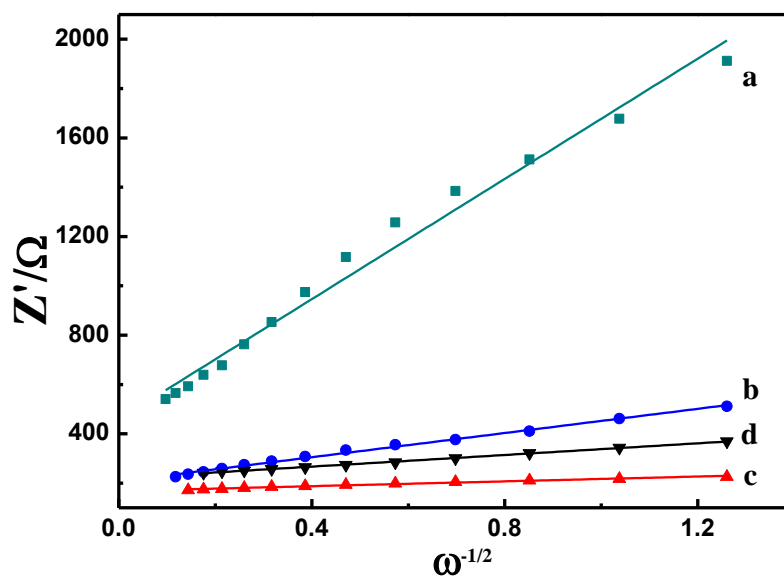
Figure 9. The typical curves describing the relationship between Z' and $\omega^{-1/2}$. Curve a, b, c and d were for the half-cells prepared by sample a, b, c and d.

Also, the values of the Li-ion diffusion coefficient of these four samples can be evaluated using the following equation [21, 22]

$$D_{Li} = \frac{(RT)^2}{2(An^2F^2C_{Li}\sigma)^2} \qquad (1)$$

In above equation, A, n, R, T, F, C_{Li} and σ corresponded to the surface area of the electrode, the number of electrons transferred, the gas constant, the absolute temperature, the Faraday constant, the concentration of lithium ion in solid and the Warburg factor, respectively[22]. Evidently, in above equation A, R, T and F were known, and the exact values of n, C_{Li} and σ were unknown to us. Meanwhile, the value of σ could be roughly estimated using the following equation [23].

$$Z_{re} = R_s + R_{ct} + \sigma\,\omega^{-1/2} \qquad (2)$$

In above equation, Z_{re}, R_s, R_{ct} and ω stood for the real part of the impedance (here was Z'), the resistance of electrolyte, the charge transfer resistance and the angular frequency in the low frequency region, respectively. That is to say, the value of σ could be calculated from the slope of the line describing the relationship between Z_{re} and the reciprocal root square of the lower angular frequencies ($\omega^{-1/2}$). The typical curves of Z_{re} (here was Z') against $\omega^{-1/2}$ for these four samples are given in Fig. 9. According to the equations (1) and (2), it is clear that the smaller value of σ will generate a larger value of D_{Li}. To simplify the analysis, it was supposed that the values of n and C_{Li} were identical in above four samples. Therefore, the values of D_{Li} could be compared approximately, namely, the lithium diffusion coefficients for electrode a, b, c and d were in the following decreasing order, i.e., c > d >b >a. This sequence was roughly consistent with the electrochemical performance order shown in Fig.5. That is to say, sample c delivered the largest lithium diffusion coefficient among all the samples, which just interpreted the fact that the best electrochemical performance was displayed by sample c. The result of Fig.9 substantially demonstrated that the lithium diffusion behavior could be well promoted by the doped graphene.

Why did sample c exhibit the best electrochemical performance among all the prepared samples? As discussed in the results of Fig.1 and Fig.3, elementary Si, SnO_2 and graphene were the main components of sample c. In all samples, the presence of elementary Si was firmly confirmed by the XRD patterns (Fig.1). After the introduction of $SnCl_4$, the particle size of Si was greatly enlarged which meant that some prepared SnO_2 particles were coated on the surface of Si. Thus, a core-shell structure was created, in which Si was used as the core and the newly formed SnO_2 acted as the shell. Meanwhile, in the preparation process of SnO_2, most part of oxygen gas in the air was consumed, and as a result, some pieces of graphene were left and were not converted to be CO_2. Due to the presence of graphene in sample c, thus, a novel structure, namely, core-shell and sandwich structure, was tentatively proposed as shown in Fig.10.

In Fig.10, the elementary Si particles acted as strong pillars, by which the doped materials of graphene were separated piece by piece. As a result, more space was created which was very advantageous to the flowing of the electrolyte. As reported previously, SnO_2 could be employed as anode materials for LIBs. Therefore, the electrolyte in these newly created spaces could react with both graphene and SnO_2, as a result, higher capacity value was obtained. That is to say, more contacting

areas between the anode material and the electrolyte were generated by the erected Si particles, which would greatly low down the over-potential of lithiation and delithiation process. Consequently, the smallest R_{ct} value and the largest lithium diffusion coefficient were exhibited by sample c, delivering the best electrochemical performance among all prepared samples.
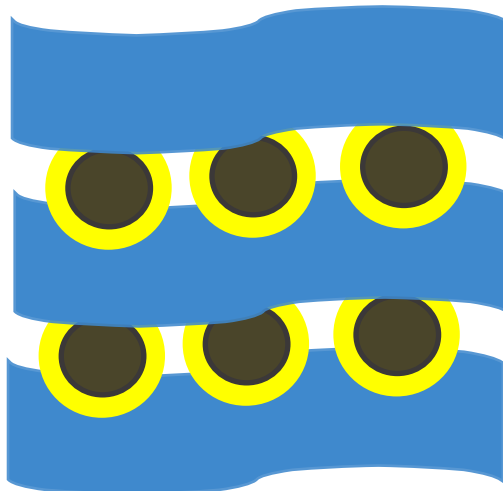
Figure 10. The structure schematic diagram for sample c, in which the black particle stood for the elementary Si, the yellow layer represented the formed SnO_2, and the blue ribbon corresponded to graphene.

4. CONCLUSION

　　　In this work, four kinds of samples, i.e., Si (sample a), Si+$SnCl_4$ (sample b), Si+$SnCl_4$+graphene (sample c) and Si+$SnCl_4$+lignin (sample d), were prepared by using a very simple method of an air condition calcination method employing commercial silicon wafer, $SnCl_4$ and graphene as the starting materials. XRD results indicated that elementary Si existed in all prepared samples and $SnCl_4$ was converted into SnO_2 in the final samples. Electrochemical measurement results indicated that the discharge capacity of sample c was estimated to be about 350 mAh g^{-1} after 20 cycles at 100 mA g^{-1}, which was greatly larger than the theoretical capacity value of anode material LTO. Also, the significant role of graphene in enhancing the electrochemical performance of the resultant samples was well demonstrated in this work. And a novel structure, namely, core-shell and sandwich structure, was proposed to explain the satisfactory electrochemical performance displayed by sample c. It should be emphasized that in the preparation of sample c, no critical preparation conditions were employed. Thus, sample c can be easily large-scale produced, which was very meaningful to the commercial production of LIBs anode materials.

References

1. B. Wang, Z. Wen, J. Jin, X. Hong, S. Zhang and K. Rui, *J. Power Sources*, 342 (2017) 521.
2. X. Lu, L. Gu, Y. S. Hu, H. C. Chiu, H. Li, G. P. Demopoulos and L. Chen, *J. Am. Chem. Soc.,* 137 (2015) 1581.
3. H. Shi, A. Yuan and J. Xu, *J. Power Sources,* 364 (2017) 288.
4. S. W. Kim, D. T. Ngo, J. Heo, C. N. Park and C. J. Park, *Electrochim. Acta,* 238 (2017) 319.
5. L. Zhang , G. L. Xia, Z. Guo, D. Sun, X. Li and X. Yu, *J. Power Sources,* 324 (2016) 294.
6. Z. Wang, L. Zhou and X. W. Lou, *Adv. Mater,* 24 (2012) 1903.
7. Z. Yi, Q. Han, D. Geng, Y. Wu, Y. Cheng and L. Wang, *J. Power Sources,* 342 (2017) 861.
8. R. Liu, D. Li, C. Wang, N. Li, Q. Li, X. Lü, J. S. Spendelow and G. Wu, *Nano Energy,* 6 (2014) 73.
9. D. Cui, Z. Zheng, X. Peng, T. Li, T. Sun, L. Yuan, *J. Power Sources,* 362 (2017) 20.
10. S. Cho, H. Y. Jang, I. Jung, L. Liu and S. Park, *J. Power Sources,* 362 (2017) 270.
11. T. Kasukabe, H. Nishihara, S. Iwamura and T. Kyotani, *J. Power Sources,* 319 (2016) 99.
12. F. Lyu, Z. Sun, B. Nan, S. Yu, L. Cao, M. Yang, M. Li, W. Wang, S. Wu, S. Zeng, H. Liu and Z. Lu, *ACS Appl. Mater. Interfaces,* 9 (2017) 10699.
13. K. Ding, Y. zhao, L. Liu, Y. Li, L. Liu, L. Wang, X. He and Z. Guo, *Electrochim. Acta*, 176 (2015) 240.
14. K. Ding, J. Zhao, J. Zhou, Y. Zhao, Y. Chen, L. Liu, L. Wang, X. He and Z. Guo, *Mater. Chem. Phy.*, 177 (2016) 31.
15. K. Ding, H. Gu, C. Zheng, L. Liu, L. Liu, X. Yan and Z. Guo, *Electrochim. Acta,* 146 (2014) 585.
16. M. Gauthier, D. Reyter, D. Mazouzi, P. Moreau, D. Guyomard, B. Lestriez and L.l Roué, *J. Power Sources,* 256 (2014) 32.
17. Q. Guo, Z. Zheng, H. Gao, J. Ma and X. Qin, *J. Power Sources*, 240 (2013) 149.
18. K. Ding, J. Zhao, J. Zhou, Y. Zhao, Y. Chen, Y. Zhang, B. Wei, L. Wang and X. He, *Int. J. Electrochem. Sci*., 11 (2016) 446.
19. K. Ding, Y. Zhao, M. Zhao, Y. Li, J. Zhao, Y. Chen and Q. Wang, *Int. J. Electrochem. Sci.,* 10 (2015) 7917.
20. G. Q. Zhang, W. Li, H. Yang, Y. Wang, S. B. Rapole, Y. Cao, C. Zheng, K. Ding and Z. Guo, *J. New Mat. Electr. Sys.*, 16 (2013) 25.
21. K. Ding, J. Zhao, Y. Sun, Y. Chen, B. Wei, Y, Zhang and J. Pan, *Ceram. Int.*, 42 (2016) 19187.
22. A. Y. Shenouda and H. K. Liu, *J. Power Sources,* 185 (2008) 1386.
23. T. F. Yi, H. Liu, Y. R. Zhu, L. J. Jiang, Y. Xie and R. S. Zhu, *J. Power Sources,* 215 (2012) 258.